EurJIC
European Journal of Inorganic Chemistry

Chemistry Europe
European Chemical Societies Publishing

Accepted Article

Title: Synthesis, Isomerization and Electrocatalytic Properties of Thiolate-Bridged Dicobalt Hydride Complexes with Different Substituents

Authors: Chunlong Wang, Jianzhe Li, Dawei Yang, Peng Tong, Puhua Sun, Baomin Wang, and Jingping Qu

To be cited as: *Eur. J. Inorg. Chem.* 10.1002/ejic.202000369

Link to VoR: https://doi.org/10.1002/ejic.202000369

WILEY-VCH

10.1002/ejic.202000369

WILEY-VCH

Synthesis, Isomerization and Electrocatalytic Properties of Thiolate-Bridged Dicobalt Hydride Complexes with Different Substituents

Chunlong Wang,[a] Jianzhe Li,[a] Dawei Yang,*[a] Peng Tong,[a] Puhua Sun,[a] Baomin Wang[a] and Jingping Qu[a][b]

Through different pathways, two unsaturated thiolate-bridged $Co^{II}Co^{II}$ complexes [Cp*Co(μ-SR)$_2$CoCp*] (**1**, R = Ph; **3**, R = ^{i}Pr, Cp* = η^5-C_5Me_5) were successfully synthesized. Interaction of complexes **1** or **3** with HBF_4 resulted in oxidative addition to give the corresponding thiolate-bridged $Co^{III}Co^{III}$ hydride bridged complexes **4[BF$_4$]** and **5[BF$_4$]**. ^{1}H NMR spectroscopic results indicate there exist two conformational isomers after protonation, in which the substituents on the thiolate ligands arranged in a symmetric or unsymmetric geometry. Interestingly, major *sym*-**4[BF$_4$]** can irreversibly convert into minor *unsym*-**4[BF$_4$]** at 30 °C evidenced by time-dependent ^{1}H NMR spectroscopy. Supprisingly, two isomers of **5[BF$_4$]** remain a dynamic equilibrium from −80 to 30 °C corroborated by variable-temperature ^{1}H NMR spectra. Furthermore, these thiolate-bridged dicobalt hydride complexes are proved to be catalysts for electrocatalytic proton reduction by cyclic voltammetry. Notably, complex **5[BF$_4$]** exhibits better catalytic activity, which highlights the importance of the flexibility of the auxiliary ligand.

Introduction

Hydrogen as a sustainable and environmentally friendly energy source, is widely considered as a potential desired alternative of increasingly exhausted fossil fuel.[1] In this context, the development of various H_2-evolving catalysts based on transition metals constitutes an attractive subject of great importance.[2] Of the most majority of the catalytic systems, irrespective of homo- or heterogeneous, those based on the noble metal platinum have proven to be the most efficient and robust.[3] However, owing to the scarcity and high cost of platinum, it is almost unavailable for large-scale applications for hydrogen production. Hence, catalysts for hydrogen evolution involving inexpensive earth-abundant transition metals such as iron, cobalt, and nickel have drawn increasing attention.[4] In contrast with catalysts containing iron and nickel inspired by biological [FeFe]- and [NiFe]-hydrogenases,[5] Co-based H_2-evolving catalysts emerged late but developed rapidly in the past two decades due to its rich and affordable redox behaviour between the Co^{3+}, Co^{2+} and Co^{+} states.

So far, a number of Co-based catalysts have been reported for H_2 evolution supported by various ligands, such as diglyoxime[6], functionalized porphyrin[7], polypyridyl[8] and other macrocycle[9] donors. To the best of our knowledge, most of these cobalt-based catalysts are mononuclear, and only a few catalytic systems involved dinuclear cobalt complexes.[10] For example, Fukuzumi and co-workers adopted multidentate ligands containing nitrogen donors to obtain a dicobalt complex $[Co_2(trpy)_2(\mu\text{-bpp})(OH)(OH_2)]^{4+}$ (trpy = terpyridine, bpp = bis(pyridyl)pyrazolato), which can promote proton reduction to release hydrogen.[10c] Whether in homolytic or heterolytic pathway, the dicobalt hydride species was believed to be the essential intermediate during H_2 formation. Consequently, synthesis of dicobalt hydride complexes is pivotal to get deep insight into the detailed mechanism based on the dicobalt centers.

On the other hand, compared with commonly used nitrogen ligands, soft weak-field sulphur ligand was scarcely applied for active cobalt-based catalysts. In hydrogenases[11] and some biomimetic bimetallic models[12], flexible thiolate ligands play a key role in that its mobility can lead to the conformational change of overall molecular structure to accommodate the protonation and subsequent hydrogen generation. Nonetheless, this similar phenomenon was never observed in the bioinspired dicobalt systems.

In our preliminary work, we utilized a rigid bidentate benzene-1,2-dithiolate (bdt) as the bridging ligand to construct a series of homo- or hetero bimetallic complexes [Cp*M(μ-bdt)MCp*] (M = Fe, Co, Ru, Rh; Cp* = η^5-C_5Me_5), which exhibit versatile reactivity toward biomimetic nitrogen fixation and small molecule activation.[13] Some related bimetallic hydride complexes can serve as active catalysts for proton reduction to hydrogen.[10f,13b] Notably, the bidentate bdt ligand is completely stationary during the formation process of the dicobalt hydride bridged complex through protonation, which may be unfavorable for subsequent catalytic hydrogen generation.

As an extension of our work, herein we modify the rigid bridging ligand to flexible mono-dentate thiolates with different substituents. Protonation studies demonstrate there exist two main protonated isomers with obviously distinct geometric arrangements in solution. When the substituent is the phenyl group, the symmetric isomer can irreversibly transform into unsymmetrical one. Interestingly, two isomers are in a dynamic equilibrium when using the isopropyl group. Importantly, dynamic mixture **5[BF$_4$]** displays more excellent catalytic

[a] C. Wang, J. Li, P. Sun, Dr. P. Tong, Dr. D. Yang, Prof. B. Wang, Prof. J. Qu
State Key Laboratory of Fine Chemicals
Dalian University of Technology
Dalian, 116024, P. R. China
E-mail: yangdw@dlut.edu.cn
URL: http://faculty.dlut.edu.cn/yangdawei/zh_CN/
[b] Prof. J. Qu
Key Laboratory for Advanced Materials
East China University of Science and Technology
Shanghai, 200237, P. R. China
Supporting information

capacity of hydrogen evolution than static complex *unsym*-**4[BF$_4$]**.

Results and Discussion

Preparation and characterization of phenyl thiolate-bridged dicobalt complex

As illustrated in **Scheme 1**, treatment of precursor complex [Cp*Co(μ-Cl)$_2$CoCp*] with 2 equiv. of NaSPh resulted in the salt metathesis reaction to smoothly give the neutral phenyl thiolate-bridged Co^{II}Co^{II} complex [Cp*Co(μ-SPh)$_2$CoCp*] (**1**) in good yield. Notably, the [Co$_2$S$_2$] framework of unsaturated complex **1** is stable under an inert gas atmosphere in solution and does not recombine to form coordinatively saturated [Co$_2$S$_3$]-type complex as observed in analogue diiron system.[14] The proton nuclear magnetic resonance (^{1}H NMR) spectrum of complex **1** displays an intense signal at δ 1.66 ppm integrating for 30 H, which can be attributed to the methyl groups in the two equivalent Cp* ligands. In addition, two very broad resonances at δ 7.10 and 7.53 ppm are attributable to the two SPh ligands, which should be obviously affected by the paramagnetic interference. This phenomenon can be reasonably explained by the experimental fact that the solution magnetic measurement of complex **1** in C$_6$D$_6$ at room temperature was measured by the Evans method to give the μ_{eff} value of 1.12 μ_B.

In good agreement with ^{1}H NMR spectroscopic results, the molecular structure of **1** is exactly symmetrical as shown in **Figure 1**. Its overall structure consists of two {Cp*Co} subunits bridged by two monodentate phenyl thiolate ligands. The dihedral angle between two phenyl groups is 15.992°, which suggests the two Ph rings tend to be in a parallel arrangement. The Co–Co distance of 2.5229(5) Å in **1** is longer than those in the bidentate thiolate-bridged dicobalt complexes [Cp*Co(μ-η^2:η^2-edt)CoCp*] (edt = ethanedithiolate)[15] and [Cp*Co(μ-η^2:η^2-bdt)CoCp*].[10f]

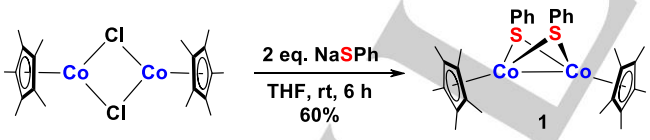

Scheme 1. Synthesis of neutral phenyl thiolate-bridged Co^{II}Co^{II} complex **1**.

Preparation and characterization of isopropyl thiolate-bridged dicobalt complexes

One step further, we have attempted to employ the alkyl thiolate as bridging ligand to construct analogue [Co$_2$S$_2$]-type complex. Differently, the isopropyl thiolate-bridged dicobalt complex was generated by a two-step synthetic pathway as described in **Scheme 2**. Firstly, the isopropyl thiolate-bridged Co^{III}Co^{III} complex [Cp*Co(I)(μ-S^{i}Pr)$_2$(CO)CoCp*][BPh$_4$] (**2**) was synthesized by the self-assembly of two half-sandwich mononuclear Co^{III} precursors in the presence of excess NaOAc followed by counter ion exchange with NaBPh$_4$. The ^{1}H NMR spectrum of **2** shows two sharp resonances at δ 1.56 and 1.64 ppm assignable to two inequivalent Cp* ligands. In addition, two doublets at δ 1.07 ppm with J = 6.8 Hz and 1.20 ppm with J = 6.6 Hz and one multiplet at δ 2.89 ppm are attributable to methyl and methine protons of the two S^{i}Pr ligands, respectively. The ^{1}H NMR data clearly indicates the two cobalt centers should be in different chemical environments. The electrospray ionization high-resolution mass spectrometry (ESI-HRMS) reveals one major molecular ion peak [**2**−BPh$_4$]$^+$ with an *m/z* of 693.0547 (calcd 693.0542) and the other minor signal peak [**2**−BPh$_4$−CO]$^+$ with an *m/z* of 665.0590 (calcd 665.0593), indicating the existence of an iodo group and a weakly coordinated carbonyl ligand in **2**.

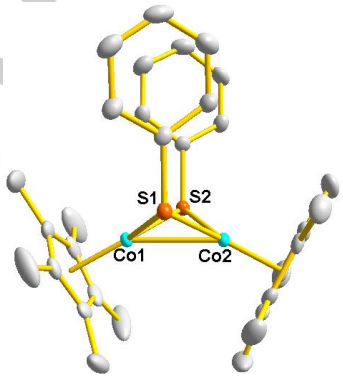

Figure 1. Molecular structure of **1**. The thermal ellipsoids are shown at the 50% probability. All hydrogen atoms are omitted for clarity.

Meanwhile, in the infrared (IR) spectrum of **2**, a notable absorbance appears at 2014 cm^{-1}, which is attributed to the stretching vibration of the terminal carbonyl ligand. Compared with other cobalt CO complexes,[16] its relatively high wavenumber suggests the weaker transfer of back-bonding electron density from Co center to π* orbitals of CO. An ORTEP drawing of **2** is shown in **Figure S2**. The two isopropyl thiolate ligands are bridged between the two {Cp*Co} subunits and the remaining coordination sites of the two cobalt centers are occupied by one iodide and one carbonyl, respectively. The distance between the two Co centers of 3.3406(1) Å is obviously longer than most of the reported dicobalt complexes.[17]

Subsequently, treatment of **2** with 2 equiv. of CoCp$_2$ resulted in two successive one-electron reduction processes to generate the neutral isopropyl thiolate-bridged Co^{II}Co^{II} complex [Cp*Co(μ-S^{i}Pr)$_2$CoCp*] (**3**) in good yield accompanied with dissociation of iodo and CO (**Scheme 2**). The ^{1}H NMR spectrum of **3** in CD$_2$Cl$_2$ shows an intense resonance at δ 1.72 ppm for two equivalent Cp* methyl protons. Besides, one diagnostic doublet at δ 1.21 ppm with J = 6.2 Hz and one broad peak at δ 0.99 ppm are attributable to the methyl and methine protons of the two equivalent S^{i}Pr ligands, respectively. The solid-state structure of **3** as shown in **Figure 2** was very similar to complex **1**. There are also containing a butterfly-type Co$_2$S$_2$ core framework featuring a symmetrical geometric arrangement. Orientational disorder of

the two isopropyl substituents leads to equivalence as observed in its ^{1}H NMR spectrum. Strikingly, similar situation was not found in its analogue possessing ethyl substituent.[18]

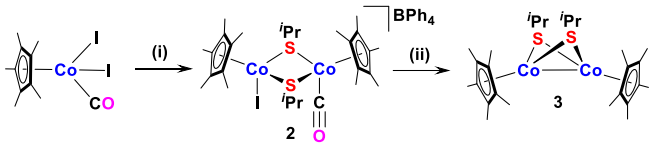

Scheme 2. Synthetic pathway of isopropyl thiolate-bridged $Co^{II}Co^{II}$ complex **3**. *Reagents and conditions*: (i) 4 equiv. of ^{i}PrSH, 10 equiv. of NaOAc, 0.6 equiv. of $NaBPh_4$, CH_2Cl_2:H_2O = 1:1, rt, 6 h, 72%; (ii) 2 equiv. of $CoCp_2$, CH_2Cl_2, −78 °C to rt, 70%.

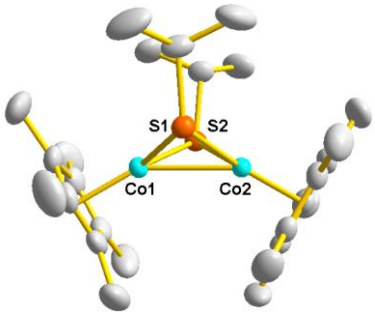

Figure 2. Molecular structure of **3**. The thermal ellipsoids are shown at the 50% probability. All hydrogen atoms are omitted for clarity.

Protonation studies of complexes 1 and 3

Next, in order to obtain thiolate-bridged dicobalt hydride complexes as key intermediate during proton reduction to hydrogen, we explored the protonation behaviors of complexes **1** and **3**. Treatment of **1** with 1 equiv. of $HBF_4{\cdot}Et_2O$ from −78 °C to room temperature led to the oxidative addition to give a mixture of *sym*-[Cp*Co(*μ*-SPh)$_2$(*μ*-H)CoCp*][BF_4] (*sym*-**4[BF$_4$]**) as the main product and *unsym*-[Cp*Co(*μ*-SPh)$_2$(*μ*-H)CoCp*][BF_4] (*unsym*-**4[BF$_4$]**) as the minor one (**Scheme 3**). The ^{1}H NMR spectrum of **4[BF$_4$]** in CD_2Cl_2 clearly shows two sets of proton resonances for two isomers. A sharp resonance at *δ* 1.39 ppm for Cp* and one diagnostic resonance at *δ* −15.88 ppm for bridging hydride are attributable to the symmetrical isomer. Corresponding proton signals at *δ* 1.62 and −14.71 ppm are assigned to the unsymmetrical one. In contrast with reported dicobalt hydride bridged complexes,[10c,10f,19] the bridging hydride signals appear in the higher field region. There is no way to distinguish these two isomers in the ESI-HRMS, because only one molecular ion peak for [**4**]$^+$ with an *m/z* of 607.1315 (calcd 607.1313) was observed. However, ESI-HRMS data can provide enough evidence for the existence of the hydride ligand.

Through further purification by recrystallization, complex *sym*-**4[BF$_4$]** with relatively high purity can be obtained, in which there are still a small amount of complex *unsym*-**4[BF$_4$]**. Single-crystals of complex *sym*-**4[BF$_4$]** were easily obtained in the suitable double-solvent system, and its symmetrical molecular structure was confirmed by X-ray diffraction analysis as shown in **Figure 3a**. Notably, the hydride of *sym*-**4[BF$_4$]** is located in the Fourier difference map, which serves as a bridging ligand between two cobalt centers. After protonation, the two phenyl groups remarkably flip down in opposite directions. Unexpectedly, the dihedral angle of nonplanar Co_2S_2 core decreases from 128.413(3)° in **1** to 99.225(3)° instead (**Table 1**). Meanwhile, the two Cp* rings turn upward with the significant

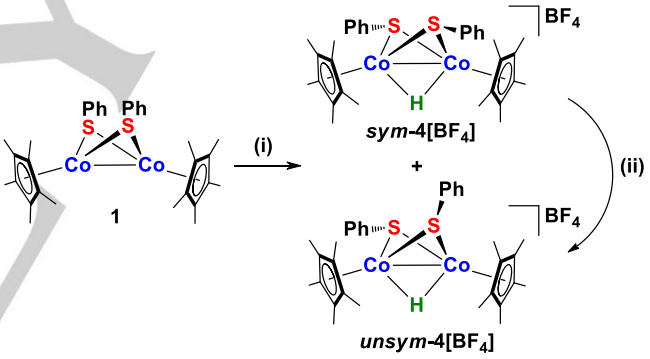

Scheme 3. Protonation of phenyl thiolate-bridged $Co^{II}Co^{II}$ complex **1**. *Reagents and conditions*: (i) 1 equiv. of $HBF_4{\cdot}Et_2O$, CH_2Cl_2, −78 °C to rt, 70% of *sym*-**4[BF$_4$]**; (ii) CH_2Cl_2, 30 °C, 5 h, 90% based on **1**.

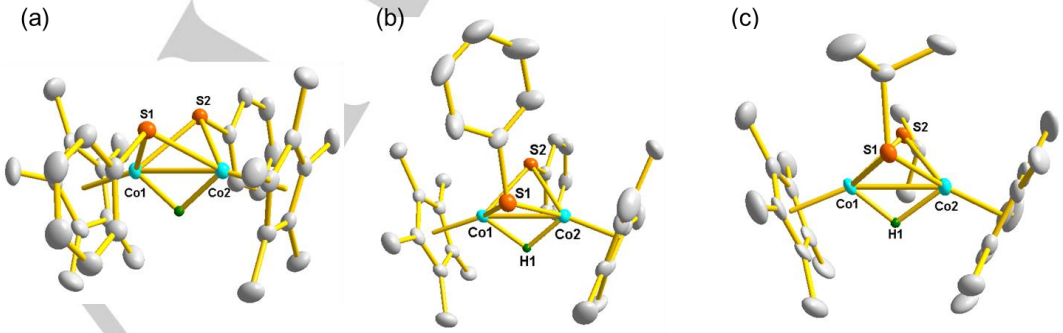

Figure 3. Molecular structures of *sym*-**4[BF$_4$]** (a), *unsym*-**4[BPh$_4$]** (b) and *unsym*-**5[BPh$_4$]** (c). The thermal ellipsoids are shown at the 50% probability. Hydrogen atoms except for the bridging hydride between two Co centers and counter anions are omitted for clarity.

decrease of the dihedral angle between them from 55.232° in **1** to 28.719°. As expected, the Co1–Co2 distance of 2.4998(7) Å is shortened compared with precursor complex **1**.

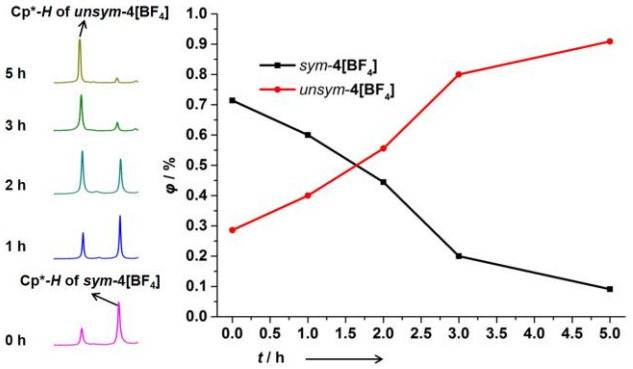

Figure 4. The time-dependent ^{1}H NMR spectra of conversion from *sym*-**4[BF$_4$]** to *unsym*-**4[BF$_4$]** over 5 h in CD_2Cl_2 at 30 °C. A growing signal at δ 1.62 ppm for Cp*-*H* of *unsym*-**4[BF$_4$]** was observed with the signal at δ 1.39 ppm for Cp*-*H* of *sym*-**4[BF$_4$]** decreased to determine the conversion of two isomers.

In order to confirm whether there exists an interconversion between the two isomers in solution or not, the time-dependent ^{1}H NMR studies for the mixture of the two isomers at 30 °C were performed. As illustrated in **Figure 4**, integral area of the singlets for Cp* was chosen for determining the genuine ratio of the two isomers in solution. At the beginning, *sym*-**4[BF$_4$]** exists as a dominant species in solution state. As time goes on, the intensity of the resonance at δ 1.39 ppm for *sym*-**4[BF$_4$]** gradually weakened, in the same time, the proton signal at δ 1.62 ppm for *unsym*-**4[BF$_4$]** continuously enhanced. After 5 h, complex *sym*-**4[BF$_4$]** almost completely converted into *unsym*-**4[BF$_4$]**. On the other hand, when lowering the temperature, isomer *unsym*-**4[BF$_4$]** cannot regenerate the other isomer *sym*-**4[BF$_4$]**, which suggests this configuration switch is an irreversible process.

For comparison, we subsequently investigated the protonation properties of complex **3**. As shown in **Scheme 4**, protonation of complex **3** also generates two isomers *sym*-[Cp*Co(μ-S^{i}Pr)$_2$(μ-H)CoCp*][BF$_4$] (*sym*-**5[BF$_4$]**) and *unsym*-[Cp*Co(μ-S^{i}Pr)$_2$(μ-H)CoCp*][BF$_4$] (*unsym*-**5[BF$_4$]**). In the ^{1}H NMR spectrum, two characteristic resonances at δ −12.83 and −14.05 ppm in the high field are assigned to the bridging hydride of *sym*- and *unsym*-**5[BF$_4$]**, respectively. Different from above mentioned system, the amounts of two isomers are very close at room temperature. As shown in **Figure 5**, *in situ* variable temperature ^{1}H NMR spectra indicate the obvious variation of the proportion of the two isomers was not observed from −80 °C to 0 °C. When the temperature increased to 30 °C and maintained for 5 h, similar transforamtion as above was also not found. These experimental results clearly reveal the two isomers should be in a dynamic equilibrium in solution. Furthermore, the molecular structures of *unsym*-**4[BPh$_4$]** and *unsym*-**5[BF$_4$]** were also demonstrated by X-ray diffraction analysis. As displayed in **Figure 3b** and **3c**, their butterfly-shaped Co_2S_2 core framework are similar to the *sym*-**4[BF$_4$]** except for the two substituent groups. They are in an unsymmetrical arrangement with different stretching orientations. This phenomenon that two phenyl groups arranged in two different fashions in the two isomers was also found in dimeric cyclopentadienyl nickel amido bridged complexes,[20] however, there is no report about thiolate-bridged dicobalt complex with similar situation.

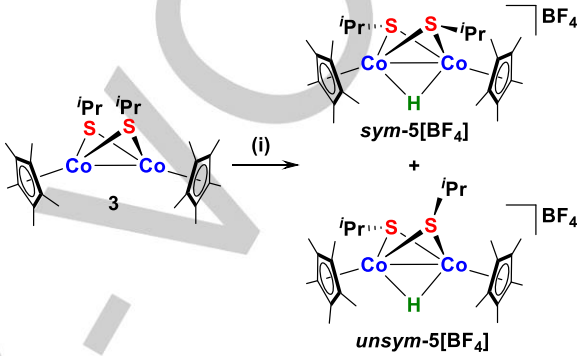

Scheme 4. Protonation study of isopropyl thiolate-bridged Co^{II}Co^{II} complex **3**. *Reagents and conditions:* (i) 1 equiv. of $HBF_4{\cdot}Et_2O$, CH_2Cl_2, −78 °C to 30 °C, 80%.

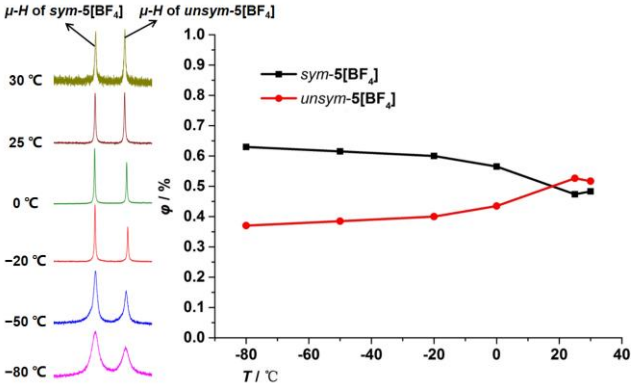

Figure 5. The *in situ* variable temperature ^{1}H NMR spectrum of protonation of **3** in CD_2Cl_2. Signals at δ −12.83 ppm for *μ-H* of *sym*-**5[BF$_4$]** and −14.05 ppm for *μ-H* of *unsym*-**5[BF$_4$]** show no obvious variation from −80 °C to 0 °C and no transforamtion of the two isomers at 30 °C for 5 h.

In these Co_2S_2 systems, the substituent on the thiolate ligand has an obvious effect on the protonation behavior. In bdt system, there is only one product; in the isopropyl system, there are two hardly convertible isomers; in the phenyl system, there are two facilely convertible isomers.

Table 1. Main bond lengths (Å) and angles (deg) in complexes **1**, **3**, *sym*-**4[BF$_4$]**, *unsym*-**4[BPh$_4$]** and *unsym*-**5[BPh$_4$]**.

Complex	**1**	**3**	*sym*-**4[BF$_4$]**	*unsym*-**4[BPh$_4$]**	*unsym*-**5[BPh$_4$]**
Co1−Co2	2.5229(5)	2.5215(5)	2.4998(7)	2.4888(5)	2.4833(7)
Co1−S1	2.1875(7)	2.1903(7)	2.2410(10)	2.2405(9)	2.2072(11)
Co1−S2	2.1968(7)	2.1950(7)	2.2347(10)	2.2345(8)	2.2197(11)
Co2−S1	2.1976(7)	2.1878(7)	2.2352(10)	2.2107(8)	2.2249(10)
Co2−S2	2.1912(7)	2.1908(7)	2.2378(10)	2.2343(8)	2.2485(10)
Co1−H1	-	-	1.6680(1)	1.6680(1)	1.6430(4)
Co2−H1	-	-	1.5760(1)	1.5760(1)	1.5273(3)
Co1−Cp*1	1.6876(1)	1.6993(1)	1.6852(1)	1.6852(1)	1.6829(3)
Co2−Cp*2	1.6832(1)	1.6947(1)	1.6813(1)	1.6813(1)	1.6852(3)
S1−Co1Co2−S2	128.413(3)	126.263(3)	99.225(3)	109.635(2)	105.139(12)
Cp*1−Cp*2	55.232	58.456	28.719	37.695	56.190

Electrochemical studies of dicobalt hydride bridged complexes

Firstly, the redox properties of two dicobalt hydride bridged complexes *unsym*-**4[BF$_4$]** and **5[BF$_4$]** in CH_2Cl_2 were explored by cyclic voltammetry (**Figure S23** and **S24**). The cyclic voltammogram of complex *unsym*-**4[BF$_4$]** displays a reversible reduction event at $E_{1/2}^{red}$ = −1.20 V versus $Fc^{+/0}$, whose reduction peak current is comparable to that of equivalent ferrocene (Fc) as an internal standard. This experimental fact implicates this reduction is a one-electron transfer process, hence, this redox couple is assigned to $Co^{III}Co^{III}/Co^{III}Co^{II}$. Similarly, the cyclic voltammogram of **5[BF$_4$]** also shows a reversible one-electron reduction process at $E_{1/2}^{red}$ = −1.30 V versus $Fc^{+/0}$, which is negatively shifted compared with *unsym*-**4[BF$_4$]**. This difference of the reductive potential is attributed to the electronic effect of the substituent in the thiolate ligand.

Subsequently, the electrocatalytic properties of complexes *unsym*-**4[BF$_4$]** and **5[BF$_4$]** for proton reduction to hydrogen were investigated by cyclic voltammetry. Upon addition of 1 equiv. of CF_3COOH (TFA) to a CH_2Cl_2 solution of **5[BF$_4$]**, a new reductive peak appeared at −1.20 V. As the acid concentration increased, the peak current of the reduction event increased linearly and the potential is shifted toward more negative cathodic value (**Figure 6**), which is diagnostic of electrocatalytic proton reduction demonstrated by cyclic voltammetry. Further evidence for the electrocatalytic process of **5[BF$_4$]** was confirmed by bulk electrolysis of 1 mM **5[BF$_4$]** in the presence of 60 mM TFA at −1.35 V. After electrolysis over 1 h period, about 1.74 μmol of H_2 was detected by gas chromatography (**Figure S29**). Moreover, in order to exclude the possibility of the electrochemical hydrogen generation promoted by some unidentified active heterogeneous materials on the electrode, we have performed the rinse test.[21] No observation of the catalytic peak suggests that the active species is metal complex in solution not heterogeneous materials deposited on the electrode (**Figure S32**). In addition, the current height of the reduction peak at −1.25 V for *unsym*-**4[BF$_4$]** grows with increasing concentration of TFA, suggesting that *unsym*-**4[BF$_4$]** can also serve as a catalyst for electrocatalytic proton reduction (**Figure S25**).

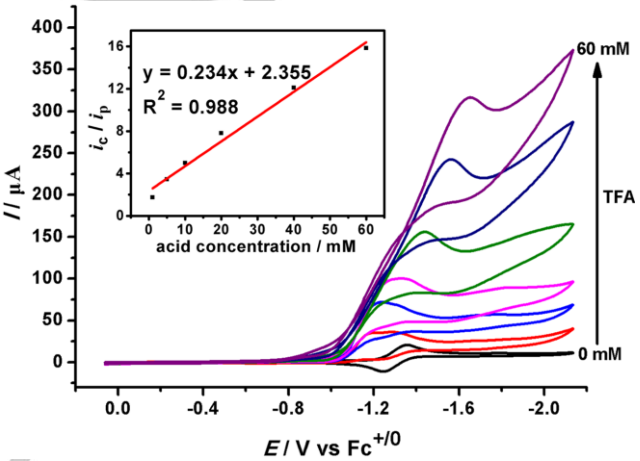

Figure 6. Cyclic voltammograms of **5[BF$_4$]** (1 mM in 0.1 M ^{n}Bu$_4$NPF$_6$ in CH_2Cl_2 under Ar) with increments of TFA (0, 1, 5, 10, 20, 40 and 60 mM)

Due to no observation of plateau currents, the foot-of-the-wave (FOTW) analysis[22] was performed to assess the catalytic capacity for *unsym*-**4[BF$_4$]** and **5[BF$_4$]**. As shown in **Figure S30**, the FOTW curves of *unsym*-**4[BF$_4$]** and **5[BF$_4$]** show a similar pattern that a steep rise followed by a constant slope. The catalytic rate constant k_{cat} values in the main domain for *unsym*-**4[BF$_4$]** and **5[BF$_4$]** are 2.68×10^2 and 5.82×10^2 M^{-1} s^{-1}, which correspond to maximum turnover frequency (TOF_{max}) of 5.37×10^2 and 11.6×10^2 s^{-1}, respectively. Hence, based on abovementioned results, we consider complex **5[BF$_4$]** is a better catalyst for electrochemical hydrogen evolution compared with *unsym*-**4[BF$_4$]**. Besides, the overpotential is another important parameter to evaluate the catalytic activity of the catalyst for hydrogen evolution, we calculated the overpotentials of dicobalt hydride bridged complexes by the updated method reported by Helm and Appel.[23] At 5 mM TFA in CH_2Cl_2, E^0_{TFA} = −0.69 V versus $Fc^{+/0}$,[24] the overpotential of *unsym*-**4[BF$_4$]** and **5[BF$_4$]** was calculated to be 0.46 and 0.43 V, respectively (**Figure S33**). At 60 mM TFA in CH_2Cl_2, the overpotential of **5[BF$_4$]** was calculated to be 0.69 V (**Figure S34**). The obvious change of

overpotential is attributable to the negative shift of potential as the increase of the acid concentration.

The catalytic activity of **5[BF_4]** is obviously superior to *unsym*-**4[BF_4]**, which may be due to the fact that the dynamic transformation in solution is beneficial to the subsequent protonation and hydrogen evolution. According to the above mentioned electronchemical results and some biomimetic diiron systems[25], we proposed the mechanism of hydrogen production is an ECEC process. Firstly, a one-electron reduction of thiolate-bridged dicobalt hydride complex took place to give a neutral hydride species, and then a protonation process occurred to give an important intermediate that the bridging thiolate ligand accepted a proton. Subsequently, the second reduction process underwent to give a metastable species containing a hydride on cobalt center and a proton on sulfur, which is followed by a rapid intramolecular proton transfer from sulfur to cobalt center to lead to the dihydrogen evolution.

Conclusions

In summary, thiolates with aliphatic or aromatic substitutent were adopted as bridging ligands to build neutral unsaturated [Co_2S_2]-type complexes **1** and **3**. Further protonation studies demonstrated the resulting dicobalt hydride bridged complexes both have two isomers in the solution state. Interestingly, when the substituent is phenyl group, the irreversible conformational conversion from symmetrical to unsymmetrical arrangement was observed in the time-dependent ^{1}H NMR spectroscopy under slight heating conditions. Distinctly, when the substituent is isopropyl group, the two isomers are nearly in a dynamic equilibrium in a very broad temperature range. Importantly, compared with complex *unsym*-**4[BF_4]** localized in solution state, structurally flexible complex **5[BF_4]** exhibits better electrocatalytic activity for proton reduction evidenced by cyclic voltammetry. Further studies on activation of other small molecules on this [Co_2S_2] platform are underway.

Experimental Section

General Procedures: All manipulations were routinely carried out under an argon or nitrogen atmosphere, using standard Schlenk techniques and glove box techniques. Unless otherwise noted, solvents were dried and deoxygenated by thoroughly sparging column in the solvent purification system by Innovative Technology, Inc. Complexes [Cp*Co(μ-Cl)$_2$CoCp*][26] and [Cp*CoI_2(CO)][27] were prepared according to the literature procedure. $CoCp_2$ (Aldrich), $HBF_4{\cdot}Et_2O$ (Energy Chemical), PhSH (Energy Chemical), ^{i}PrSH (Energy Chemical), $NaBPh_4$ (Energy Chemical), TFA (Energy Chemical) and ^{n}Bu$_4$NPF_6 (Aldrich) were commercially available and used as received without further purification.

Spectroscopic Measurements: ^{1}H NMR spectra and solution magnetic measurement measured by the Evans method were recorded on a Brüker 400 Ultra Shield spectrometer. The chemical shifts (δ) are given in parts per million relative to CD_2Cl_2 (5.32 ppm for ^{1}H), C_6D_6 (7.16 ppm for ^{1}H) and $CDCl_3$ (7.26 ppm for ^{1}H). IR data were recorded on the NEXVSTM FT-IR spectrometer. ESI-HRMS were recorded on Q-TOF Micro spectrometer. Elemental analyses were performed on a Vario EL analyzer.

Electrochemistry: Electrochemical measurements were recorded using a BAS-100W electrochemical potentiostat at a scan rate of 100 mV/s. Cyclic voltammetry experiments were carried out in a three-electrode cell under argon at room temperature. The working electrode was a glassycarbon disk (diameter 3 mm), the reference electrode was a nonaqueous Ag/Ag$^+$ electrode, the auxiliary electrode was a platinum wire, and the supporting electrolyte was 0.1 M ^{n}Bu$_4$NPF_6 in CH_2Cl_2. All potentials reported herein are quoted relative to the Fc$^+$/Fc couple. Electrocatalysis studies were performed by the addition of different amounts of TFA with microsyringe. Bulk electrolysis was performed under the same conditions as the cyclic voltammetry measurements, except that the solutions were vigorously stirred. Gas analysis was performed with a Techcomp GC7900 gas chromatography instrument with argon as the carrier gas and a thermal conductivity detector.

X-ray crystallography: The data were afforded on a Brüker SMART APEX CCD diffractometer with graphite monochromated Mo Kα radiation (λ = 0.71073 Å). Empirical absorption corrections were performed using the SADABS program.[28] All of the structures were solved by direct methods and refined by full-matrix least-squares based on all data using F^2 using SHELXTL 2014.[29] All of the non-hydrogen atoms were refined anisotropically. All of the hydrogen atoms were generated and refined in ideal positions. Full details of the X-ray structural determination are in the CIF included as Supporting Information. CCDC depositions 1989198 (**1**), 1989199 (**2**), 1989200 (**3**), 1989201 (*sym*-**4[BF_4]**), 1989202 (*unsym*-**4[BPh_4]**) and 1989203 (*unsym*-**5[BPh_4]**) can be obtained free of charge from The Cambridge Crystallographic Data Center.

Synthesis of [Cp*Co(μ-SPh)$_2$CoCp*] (1): A mixture of [Cp*Co(μ-Cl)$_2$CoCp*] (46 mg, 0.10 mmol), NaSPh (26 mg, 0.20 mmol) was stirred in THF (8 mL) at room temperature for 6 h. The resulting suspension was filtrated at room temperature, and then the filtrate was evaporated to dryness in reduced pressure. The residue was washed with MeCN for three times and extracted with CH_2Cl_2 (10 mL). A brown powder [Cp*Co(μ-SPh)$_2$CoCp*] (**1**) (36 mg, 0.06 mmol) was isolated in 60% yield after CH_2Cl_2 was removed in vacuum. Crystals of **1** suitable for X-ray diffraction were obtained from CH_2Cl_2 solution layered with MeCN at room temperature. ^{1}H NMR (400 MHz, CD_2Cl_2): δ 7.53 (br, 4H, SPh-*H*), 7.10 (br, 6H, SPh-*H*), 1.66 (s, 30H, Cp*-C*H*$_3$). Solution magnetic measurement (C_6D_6, 298 K): μ_{eff} = 1.12μ_B per dimer. IR (KBr, cm^{-1}): 3057, 2970, 2906, 1577, 1370, 1021, 735. Anal. Calcd for $C_{32}H_{40}Co_2S_2$: C, 63.35; H, 6.65. Found: C, 63.73; H, 6.31.

Synthesis of [Cp*Co(I)(μ-S^{i}Pr)$_2$(CO)CoCp*][BPh_4] (2): To a solution of [Cp*CoI_2(CO)] (476 mg, 1.00 mmol) in CH_2Cl_2 (40 mL) and H_2O (40 mL), ^{i}PrSH (304 mg, 4.00 mmol), NaOAc (820 mg, 10.00 mmol) and $NaBPh_4$ (205 mg, 0.60 mmol) were added. The color of the reaction mixture gradually changed from violet-red to green. After stirring at room temperature for 6 h, the organic phase was collected and the aqueous phase was washed with small amount of CH_2Cl_2. The combined CH_2Cl_2 solution was dried over $MgSO_4$ and filtered. The filtrate was dried under vacuum and washed with Et_2O to afford brown powder [Cp*Co(I)(μ-S^{i}Pr)$_2$(CO)CoCp*][BPh_4] (**2**) (364 mg, 0.36 mmol, 72%). Crystals of **2** suitable for X-ray diffraction were obtained from a CH_2Cl_2 solution layered with *n*-hexane at room temperature. ^{1}H NMR (400 MHz, CD_2Cl_2): δ 7.31 (br, 8H, Ph-*H*), 7.02 (t, *J* = 7.0 Hz, 8H, Ph-*H*), 6.86 (m, 4H, Ph-*H*), 2.89 (m, 2H, S-C*H*(CH$_3$)$_2$), 1.64 (s, 15H, Cp*-C*H*$_3$), 1.56 (s, 15H, Cp*-C*H*$_3$), 1.20 (d, *J* = 6.6 Hz, 6H, S-CH(C*H*$_3$)$_2$), 1.07 (d, *J* = 6.8 Hz, 6H, SCH-(C*H*$_3$)$_2$). ESI-HRMS: Calcd. For [**2**−BPh_4]$^+$ 693.0542; Found 693.0547; Calcd. For [**2**−BPh_4−CO]$^+$ 665.0593; Found 665.0590. IR (KBr,

cm^{-1}): 2014(ν_{CO}), 2968, 1466, 1362, 685. Anal. Calcd for $C_{51}H_{64}BCo_2IOS_2$: C, 60.48; H, 6.37. Found: C, 60.13; H, 6.55.

Synthesis of [Cp*Co(μ-S^{i}Pr)$_2$CoCp*] (3): To a stirred solution of **2** (1012 mg, 1.00 mmol) in 20 mL of CH_2Cl_2 was added 2 equiv. of $CoCp_2$ (378 mg, 2.00 mmol) at −78 °C, followed by stirring from −78 °C to room temperature. The reaction mixture was stirred for 4 h at room temperature and then dried in vacuum. The residue was extracted with *n*-hexane and dried under vacuum. The residue was washed by MeCN and dried in reduced pressure to give green product [Cp*Co(μ-S^{i}Pr)$_2$CoCp*] (**3**) (377 mg, 0.70 mmol, 70%). Crystals suitable for X-ray diffraction were obtained from saturated *n*-hexane solution at −30 °C. ^{1}H NMR (400 MHz, CD_2Cl_2): δ 1.72 (s, 30H, Cp*-CH_3), 1.21 (d, J = 6.2 Hz, 12H, S-CH(CH_3)$_2$), 0.99 (br, 2H, S-CH(CH$_3$)$_2$). IR (KBr, cm^{-1}): 2959, 2905, 2853, 1443, 1369, 1019. Anal. Calcd for $C_{26}H_{44}Co_2S_2$: C, 57.98; H, 8.23. Found: C, 58.15; H, 8.31.

Synthesis of *sym*-[Cp*Co(μ-SPh)$_2$(μ-H)CoCp*][BF$_4$] (*sym*-4[BF$_4$]): To a stirred solution of **1** (61 mg, 0.10 mmol) in 6 mL of CH_2Cl_2 was added 1 equiv. of $HBF_4{\cdot}Et_2O$ dropwise at −78 °C, followed by stirring from −78 °C to room temperature. Volatiles were removed in vacuum. The residue was washed by Et_2O and dried in reduced pressure to give green product, which was a mixture of *sym*-[Cp*Co(μ-SPh)$_2$(μ-H)CoCp*][BF$_4$] (*sym*-**4[BF$_4$]**) as main product and *unsym*-[Cp*Co(μ-SPh)$_2$(μ-H)CoCp*][BF$_4$] (*unsym*-**4[BF$_4$]**) as the minor one. Then further purification by recrystallization gave highly pure *sym*-**4[BF$_4$]** (48 mg, 0.07mmol, 70%). Crystals of *sym*-**4[BF$_4$]** suitable for X-ray diffraction were obtained from a CH_2Cl_2 solution layered with *n*-hexane at room temperature. ^{1}H NMR (400 MHz, CD_2Cl_2): δ 7.76 (br, 2H, SPh-*H*), 7.34 (br, 3H, SPh-*H*), 7.22 (m, 2H, SPh-*H*), 6.98 (m, 3H, SPh-*H*), 1.39 (s, 30H, Cp*-CH_3), −15.88 (s, 1H, μ-*H*).

Synthesis of *unsym*-[Cp*Co(μ-SPh)$_2$(μ-H)CoCp*][BF$_4$] (*unsym*-4[BF$_4$]): To a stirred solution of **1** (61 mg, 0.10 mmol) in 8 mL of CH_2Cl_2 was added 1 equiv. of $HBF_4{\cdot}Et_2O$ at −78 °C, followed by stirring from −78 °C to 30 °C and maintained for 5 h. Volatiles were removed in vacuum. The residue was washed by Et_2O and dried in reduced pressure to give green product *unsym*-[Cp*Co(μ-SPh)$_2$(μ-H)CoCp*][BF$_4$] (*unsym*-**4[BF$_4$]**) (62 mg, 0.09 mmol, 90%). Crystals of *unsym*-**4[BF$_4$]** were unable to obtain using various available systems. Therefore, the anion exchange reaction of *unsym*-**4[BF$_4$]** with $NaBPh_4$ was performed. Crystals of *unsym*-**4[BPh$_4$]** suitable for X-ray diffraction were obtained from a CH_2Cl_2 solution layered with *n*-hexane at room temperature. ^{1}H NMR (400 MHz, CD_2Cl_2): δ 7.50 (m, 2H, SPh-*H*), 7.42-7.35 (m, 8H, SPh-*H*), 1.62 (s, 30H, Cp*-CH_3), −14.71 (s, 1H, μ-*H*). ESI-HRMS: Calcd. For [**4**]$^+$ 607.1313; Found 607.1315. IR (KBr, cm^{-1}): 2966, 1470, 1378, 1055, 762. Anal. Calcd for $C_{32}H_{41}BCo_2F_4S_2$: C, 55.34; H, 5.95. Found: C, 55.55; H, 5.78.

Synthesis of [Cp*Co(μ-S^{i}Pr)$_2$(μ-H)CoCp*][BF$_4$] (5[BF$_4$]): To a stirred solution of **3** (53 mg, 0.10 mmol) in 10 mL of CH_2Cl_2 was added 1 equiv. of $HBF_4{\cdot}Et_2O$ dropwise at −78 °C, followed by stirring from −78 °C to 30 °C. Volatiles were removed in vacuum. The residue was washed by Et_2O and dried in reduced pressure to give green product [Cp*Co(μ-S^{i}Pr)$_2$(μ-H)CoCp*][BF$_4$] (**5[BF$_4$]**) (50 mg, 0.08 mmol, 80%), which contained two isomers (*sym*-**5[BF$_4$]** and *unsym*-**5[BF$_4$]** with close amounts) analyzed by ^{1}H NMR. Crystals of **5[BF$_4$]** were unable to obtain using various available systems. Therefore, the anion exchange reaction of **5[BF$_4$]** with $NaBPh_4$ was performed. Crystals of *unsym*-**5[BPh$_4$]** suitable for X-ray diffraction were obtained from a CH_2Cl_2 solution layered with Et_2O at room temperature. ^{1}H NMR (400 MHz, $CDCl_3$): δ 2.41 (m, 1H, S-CH(CH$_3$)$_2$ of *unsym*-**5[BF$_4$]**), 2.13 (m, 1H, S-CH(CH$_3$)$_2$ of *unsym*-**5[BF$_4$]**), 1.84 (s, 30H, Cp*-CH_3 of *unsym*-**5[BF$_4$]**), 1.28 (d, J = 6.8 Hz, 6H, S-CH(CH_3)$_2$ of *unsym*-**5[BF$_4$]**), 1.16 (d, J = 6.8 Hz, 6H, S-CH(CH_3)$_2$ of *unsym*-**5[BF$_4$]**), −14.05 (s, 1H, μ-*H* of *unsym*-**5[BF$_4$]**); 2.22 (m, 2H, S-CH(CH$_3$)$_2$ of *sym*-**5[BF$_4$]**), 1.79 (s, 30H, Cp*-CH_3 of *sym*-**5[BF$_4$]**), 1.34 (d, J = 6.7 Hz, 12H, S-CH(CH_3)$_2$ of *sym*-**5[BF$_4$]**), −12.83 (s, 1H,μ-*H* of *sym*-**5[BF$_4$]**). ESI-HRMS: Calcd. For [**5**]$^+$ 539.1627; Found 539.1639. IR (KBr, cm^{-1}): 2964, 2913, 2858, 1449, 1379, 1053. Anal. Calcd for $C_{26}H_{45}BCo_2F_4S_2$: C, 49.85; H, 7.24. Found: C, 49.84; H, 7.20.

Acknowledgements

This work was supported by the National Natural Science Foundation of China (No. 21690064, 21571026, 21231003), the Program for Changjiang Scholars and Innovative Research Team in University (No. IRT13008), the "111" project of the Ministry of Education of China and the Fundamental Research Funds for the Central Universities (DUT19RC(3)013).

Keywords: Cobalt • S Ligands • Biomimetic Synthesis • Electrochemistry

Conflicts of interest

The authors declare no competing financial interests.

References

[1] a) J. A. Turner, *Science* **2004**, *305*, 972-974; b) T. R. Cook, D. K. Dogutan, S. Y. Reece, Y. Surendranath, T. S. Teets, D. G. Nocera, *Chem. Rev.* **2010**, *110*, 6474-6502.

[2] a) S. Fukuzumi, Y. Yamada, T. Suenobu, K. Ohkubo, H. Kotani, *Energy Environ. Sci.* **2011**, *4*, 2754-2766; b) D. L. DuBois, *Inorg. Chem.* **2014**, *53*, 3935-3960.

[3] M. K. Debe, *Nature* **2012**, *486*, 43-51.

[4] a) P. Du, R. Eisenberg, *Energy Environ. Sci.* **2012**, *5*, 6012-6021; b) M. Wang, L. Chen, L. Sun, *Energy Environ. Sci.* **2012**, *5*, 6763-6778; c) J. R. McKone, S. C. Marinescu, B. S. Brunschwig, J. R. Winkler, H. B. Gray, *Chem. Sci.* **2014**, *5*, 865-878; d) S. Fukuzumi, Y.-M. Lee, W. Nam, *Coord. Chem. Rev.* **2018**, *355*, 54-73.

[5] a) M. Y. Darensbourg, E. J. Lyon, J. J. Smee, *Coord. Chem. Rev.* **2000**, *206-207*, 533-561; b) D. J. Evans, C. J. Pickett, *Chem. Soc. Rev.* **2003**, *32*, 268-275; c) C. Tard, C. J. Pickett, *Chem. Rev.* **2009**, *109*, 2245-2274; d) T. R. Simmons, G. Berggren, M. Bacchi, M. Fontecave, V. Artero, *Coord. Chem. Rev.* **2014**, *270-271*, 127-150.

[6] a) J. L. Dempsey, B. S. Brunschwig, J. R. Winkler, H. B. Gray, *Acc. Chem. Res.* **2009**, *42*, 1995-2004; b) F. Lakadamyali, M. Kato, N. M. Muresan, E. Reisner, *Angew. Chem. Int. Ed.* **2012**, *51*, 9381-9384.

[7] a) K. Ladomenou, M. Natali, E. Iengo, G. Charalampidis, F. Scandola, A. G. Coutsolelos, *Coord. Chem. Rev.* **2015**, *304-305*, 38-54; b) W. Zhang, W. Lai, R. Cao, *Chem. Rev.* **2017**, *117*, 3717-3797.

[8] a) N. Queyriaux, R. T. Jane, J. Massin, V. Artero, M. Chavarot-Kerlidou, *Coord. Chem. Rev.* **2015**, *304-305*, 3-19; b) D. Z. Zee, T. Chantarojsiri, J. R. Long, C. J. Chang, *Acc. Chem. Res.* **2015**, *48*, 2027-2036.

[9] For examples: a) C. C. L. McCrory, C. Uyeda, J. C. Peters, *J. Am. Chem. Soc.* **2012**, *134*, 3164-3170; b) D. Moonshiram, C. Gimbert-Suriñach, A. Guda, A. Picon, C. S. Lehmann, X. Zhang, G. Doumy, A. M. March, J. Benet-Buchholz, A. Soldatov, A. Llobet, S. H. Southworth, *J. Am. Chem. Soc.* **2016**, *138*, 10586-10596; c) H.-Q. Y, H.-H. Wang, J. Kandhadi, H. Wang, S.-Z. Zhan, H.-Y. Liu, *Appl. Organometal Chem.* **2017**, *31*, e3773; d) S. Chakraborty, E. H. Edwards, B. Kandemir, K. L. Bren, *Inorg. Chem.*

2019, *58*, 16402-16410; e) G. C. Tok, A. T. S. Freiberg, H. A. Gasteiger, C. R. Hess, *ChemCatChem* **2019**, *11*, 3973-3981.

[10] a) N. K. Szymczak, L. A. Berben, J. C. Peters, *Chem. Commun.* **2009**, 6729-6731; b) C. N. Valdez, J. L. Dempsey, B. S. Brunschwig, J. R. Winkler, H. B. Gray, *Proc. Natl. Acad. Sci. U.S.A.* **2012**, *109*, 15589-15593; c) S. Mandal, S. Shikano, Y. Yamada, Y.-M. Lee, W. Nam, A. Llobet, S. Fukuzumi, *J. Am. Chem. Soc.* **2013**, *135*, 15294-15297; d) S. Kal, A. S. Filatov, P. H. Dinolfo, *Inorg. Chem.* **2014**, *53*, 7137-7145; e) C. D. Giovanni, C. Gimbert-Suriñach, M. Nippe, J. Benet-Buchholz, J. R. Long, X. Sala, A. Llobet, *Chem. Eur. J.* **2016**, *22*, 361-369; f) P. Tong, W. Xie, D. Yang, B. Wang, X. Ji, J. Li, J. Qu, *Dalton Trans*. **2016**, *45*, 18559-18565; g) K. K. Kpogo, S. Mazumder, D. Wang, H. B. Schlegel, A. T. Fiedler, C. N. Verani, *Chem. Eur. J.* **2017**, *23*, 9272-9279.

[11] a) J. C. Fontecilla-Camps, A. Volbeda, C. Cavazza, Y. Nicolet, *Chem. Rev.* **2007**, *107*, 4273-4303; b) W. Lubitz, H. Ogata, O. Rüdiger, E. Reijerse, *Chem. Rev.* **2014**, *114*, 4081-4148.

[12] a) M. Schmidt, S. M. Contakes, T. B. Rauchfuss, *J. Am. Chem. Soc.* **1999**, *121*, 9736-9737; b) E. J. Lyon, I. P. Georgakaki, J. H. Reibenspies, M. Y. Darensbourg, *J. Am. Chem. Soc.* **2001**, *123*, 3268-3278; c) D. J. Crouthers, J. A. Denny, R. D. Bethel, D. G. Munoz, M. Y. Darensbourg, *Organometallics* **2014**, *33*, 4747-4755.

[13] a) Y. Li, Y. Li, B. Wang, Y. Luo, D. Yang, P. Tong, J. Zhao, L. Luo, Y. Zhou, S. Chen, F. Cheng, J. Qu, *Nat. Chem.* **2013**, *5*, 320-326; b) D. Yang, Y. Li, B. Wang, X. Zhao, L. Su, S. Chen, P. Tong, Y. Luo, J. Qu, *Inorg. Chem.* **2015**, *54*, 10243-10249; c) X. Zhao, D. Yang, Y. Zhang, B. Wang, J. Qu, *Chem. Commun.* **2018**, *54*, 11112-11115.

[14] Y. Chen, Y. Zhou, J. Qu, *Organometallics* **2008**, *27*, 666-671.

[15] S. Drobnik, C. Stoll, H. Nöth, K. Polborn, W. Hiller, I.-P. Lorenz, *Z. Naturforsch.* **2006**, *61b*, 1365-1376.

[16] a) M. H. Al-Afyouni, E. Suturina, S. Pathak, M. Atanasov, E. Bill, D. E. DeRosha, W. W. Brennessel, F. Neese, P. L. Holland, *J. Am. Chem. Soc.* **2015**, *137*, 10689-10699; b) M. M. Deegan, J. C. Peters, *Chem. Commun.* **2019**, *55*, 9531-9534.

[17] a) X. Xu, G. Jiao, H. Sun, X. Li, *Z. Anorg. Allg. Chem.* **2011**, *637*, 430-435; b) S. J. Tereniak, R. K. Carlson, L. J. Clouston, V. G. Young, E. Bill, R. Maurice, Y.-S. Chen, H. J. Kim, L. Gagliardi, C. C. Lu, *J. Am. Chem. Soc.* **2014**, *136*, 1842-1855; c) M. Gennari, B. Gerey, N. Hall, J Pécaut, M.-N. Collomb, M. Rouzières, R. Clérac, M. Orio, C. Duboc, *Angew. Chem. Int. Ed.* **2014**, *53*, 5318-5321; d) R. H. D. Lyngdoh, H. F. Schaefer III, R. B. King, *Chem. Rev.* **2018**, *118*, 11626-11706.

[18] H. Wu, J. Li, D. Yang, P. Tong, J. Zhao, B. Wang, J. Qu, *Inorg. Chem. Front.* **2019**, *6*, 2185-2193.

[19] D. J. Elliot, D. G. Holah, A. N. Hughes, H. A. Mirza, E. Zawada, *J. Chem. Soc., Chem. Commun.* **1990**, 32-33.

[20] P. L. Holland, R. A. Andersen, R. G. Bergman, *J. Am. Chem. Soc.* **1996**, *118*, 1092-1104.

[21] a) V. Artero, M. Fontecave, *Chem. Soc. Rev.* **2013**, *42*, 2338-2356; b) M. Fang, M. H. Engelhard, Z. Zhu, M. L. Helm, J. A. S. Roberts, *ACS Catal*. **2014**, *4*, 90-98.

[22] a) C. Costentin, S. Drouet, M. Robert, J.-M. Savéant, *J. Am. Chem. Soc*. **2012**, *134*, 11235-11242; b) R. Zaffaroni, R. J. Detz, J. I. van der Vlugt, J. N. H. Reek, *ChemSusChem* **2018**, *11*, 209-218.

[23] A. M. Appel, M. L. Helm, *ACS Catal.* **2014**, *4*, 630-633.

[24] a) V. Fourmond, P. A. Jacques, M. Fontecave, V. Artero, *Inorg. Chem.* **2010**, *49*, 10338-10347; b) M. D. Sampson, C. P. Kubiak, *Inorg. Chem.* **2015**, *54*, 6674-6676.

[25] a) C. Greco, G. Zampella, L. Bertini, M. Bruschi, P. Fantucci, L. De Gioia, *Inorg. Chem.* **2007**, *46*, 108-116; b) K.-T. Chu, Y.-C. Liu, Y.-L. Huang, C.-H. Hsu, G.-H. Lee, M.-H. Chiang, *Chem. Eur. J.* **2015**, *21*, 10978-10982; c) S. Ding, P. Ghosh, A. M. Lunsford, N. Wang, N. Bhuvanesh, M. B. Hall, M. Y. Darensbourg, *J. Am. Chem. Soc.* **2016**, *138*, 12920-12927.

[26] U. Koelle, B. Fuss, M. Belting, E. Raabe, *Organometallics* **1986**, *5*, 980-987.

[27] S. A. Frith, J. L. Spencer, *Inorg. Synth.* **1985**, *23*, 15-21.

[28] G. M. Sheldrich, *SADABS, Program for area detector absorption correction, Institute for Inorganic Chemistry*, University of Göttingen, Germany, **1996**.

[29] a) G. M. Sheldrick, *SHELXL-2014, Program for refinement of crystal structures*, University of Göttingen, Germany, **2014**; b) G. M. Sheldrick, *SHELXS-2014, Program for solution of crystal structures*, University of Göttingen, Germany, **2014**.

Table of Content

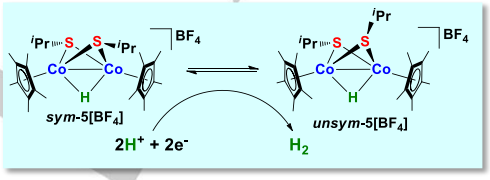

A fascinating dynamic equilibrium of conformational isomerization was observed in an alkyl thiolate-bridged dicobalt hydride complex, which is proved to be a catalyst for proton reduction to hydrogen evolution.

Key Topic: Hydrides